07,10,13

Melting criteria for classical and quantum crystals

© M.N. Magomedov

Institute for geothermal problems and renewable energy — branch of the joint Institute of high temperatures of the Russian Academy of Sciences,
Makhachkala, Russia

E-mail: mahmag4@mail.ru

Received July 19, 2024
Revised October 2, 2024
Accepted October 3, 2024

It was shown that the Lindemann ratio (L) can be calculated by means of the delocalized criterion of melting for classical crystals, i.e. those with a melting point (T_m) greater than the Debye temperature (Θ): $T_m/\Theta > 1.5$. It was shown that for classical single-component crystals, the L value is determined only by the crystal structure. Calculations for various structures of classical crystals showed good agreement with the estimates of other authors. A generalization of the Lindemann relation was obtained for the case of quantum single-component crystals, i.e. for which $T_m/\Theta < 0.4$. It was shown that for quantum crystals, the Lindemann ratio is determined not only by the crystal structure, but also by the function Θ/T_m. Therefore, when moving from the classical to the quantum domain, the $T_m(\Theta)$ function changes its functional dependence. It was shown that for quantum crystals, the L value decreases with increasing pressure along the melting line. For quantum nanocrystals, the L value increases with an isobaric decrease in the size of the nanocrystal. At the same time, the more noticeably the shape of the quantum nanocrystal deviates from the energy-optimal shape, the greater the sized increase in the Lindemann ratio. A generalization of the delocalized criterion of melting was obtained for the case of quantum single-component crystals.

Keywords: melting, delocalization, Debye temperature, quantum crystal, nanocrystal, hydrogen, helium.

DOI: 10.61011/PSS.2024.11.60099.200

1. Introduction

Various phenomenological criteria are used to calculate the properties of a crystal in case of melting because there is no theory of the crystal-liquid (C–L) phase transition (PT) yet (as there is no theory of the liquid state) [1–3]. The most widely used of these is the Lindemann melting criterion, which states the following [4,5]: the standard deviation of an atom $\langle u^2\rangle^{1/2}$ in a crystal related to the distance between the centers of the nearest atoms (c) at the melting point (T_m) of a single-component crystal is a constant value.

Lindemann believed that the ratio $\langle u^2\rangle^{1/2}/c$ is constant for all single-component crystals at T_m. However, Gilvarry using the Debye-Waller theory showed that the Lindemann ratio is constant only for crystals with the same structure [5]. Gilvarry estimates that for metals with face-centered cubic (fcc), hexagonal close-packed (hcp), and body-centered cubic (bcc) structures the Lindemann ratio at low pressure ($P = 0$) is equal to [6]:

$$L = \left(\frac{\langle u^2\rangle^{1/2}}{c}\right)_{T_m} = 0.11(fcc), 0.09(hcp), 0.13(bcc). \quad (1)$$

Various methods were proposed for estimating the value of L after Gilvarry. The values of L were obtained in the works of various authors, which slightly differ from the values of (1). The results of some work on estimating the value of L are presented in Table 1, where the author is indicated in the first column-the year and method of calculation, and the last column contains a link to the article by this author.

The dependence of the value of L on the position of the metal in the group of the Periodic table of elements has been recently studied in the paper [10] using experimental data for the ratio T_m/Θ^2. Here Θ — Debye temperature. An average value of L was obtained for 12 metal groups in paper [10]. It is in the range:

$$L = 0.07 \text{ (group 9 : } hcp\text{-Co, } fcc\text{-Rh, Ir)}$$

$$-0.139 \text{ (group 1 : } bcc\text{-Li, Na, K, Rb, Cs).}$$

Thus, the value of L for metals can widely vary depending on the used method of calculation of $\langle u^2\rangle$: from 0.07 to 0.183.

The Lindemann ratio has been studied in many papers by various methods for four fcc crystals of inert gases. This is due to the fact that atoms of inert gases have a filled outermost electron shell, i.e. they are electron-neutral and spherically symmetric. The values of L from Refs. [11–16] are listed in Table 2. The author–the year and the link to the article are indicated in first line, and the method of calculating the value of L is indicated in the bottom line.

The lattice dynamics method was used in Ref. [11] for atoms interacting through a paired 4-parameter Mie-

Table 1. The Lindemann ratio at $T_m(P = 0)$ for metals from Refs. [7–9]

Authors–year Method	*fcc*	*hcp*	*bcc*	Ref.
Shapiro–1970 Lattice dynamics method	0.071		0.113	[7]
Cho–1982 Method of harmonic atoms vibration	0.09659–0.1183	0.06886–0.08433	0.1210–0.1483	[8]
Matsuura et al.–2010 Nearly free electron model	0.172		0.183	[9]

Table 2. Lindemann ratio at $T_m(P = 0)$ for *fcc* crystals of Ne, Ar, Kr, and Xe

Crystal	Goldman–1969 [11]		Gupta–1973 [12]	Crawford–1977 [13]	Singh & Neb–1984 [14]	Mohazzabi & Behroozi–1987 [15]	Batsanov–2009 [16]
Ne	0.156–0.155	0.109–0.105	0.1446	0.127	0.202	0.148	0.113–0.114
Ar	0.130–0.128	0.101–0.097	0.1149	0.113	0.151	0.122	0.103–0.132
Kr	0.127–0.126	0.100–0.096	0.1129	0.115	0.142	0.110	0.103–0.125
Xe	0.125–0.122	0.099–0.095	0.0992	0.114	0.142	0.106	0.102–0.133
Method	Quasi-harmonic $(b = 12)$–$(b = 13)$	Anharmonic $(b = 12)$–$(b = 13)$	Quasi-harmonic approximation	From entropy data	With account three-body interactions	By Einstein model and potential $a = 6$ and $b = 12$	By thermodynamic data and own model

Lennard-Jones potential, which has the following form:

$$\phi(r) = \frac{D}{(b-a)}\left[a\left(\frac{r_0}{r}\right)^b - b\left(\frac{r_0}{r}\right)^a\right], \qquad (2)$$

where D and r_0 — depth and coordinate of the minimum potential, $b > a > 1$ — parameters.

The „only nearest neighbors interaction“ approximation was used to calculate the value $\langle u^2\rangle$ in Ref. [11], and the calculations were performed both in the quasi-harmonic approximation (first column) and taking into account the anharmonicity of atomic vibrations (second column). At the same time the following exponents of potential (2) were taken: $a = 6$, $b = 12$ (the first value in the row) and $a = 6$, $b = 13$ (the second value in the row). A quasi-harmonic approximation was used in Ref. [12], the interatomic potential was taken as the Buckingham function, and the interaction up to the 12th coordination sphere was taken into account. The three-particle interaction of atoms was taken into account in Ref. [14]. The value of $\langle u^2\rangle$ was calculated in Ref. [15] from the shape of the potential (2) with powers $a = 6$ and $b = 12$, and atomic vibrations were taken into account according to the Einstein model. A proprietary thermodynamic method for calculating the value $\langle u^2\rangle$ was developed in Ref. [16]. As can be seen from Table 2 in all calculation methods from the papers [11–18] the value L increases with a decrease of the mass of the atom, i. e. with an increase of the quantum effects in the energy of the crystal, as noted in the articles in Refs. [17,18].

It should be noted that the criterion (1) was originally applied in Refs. [4–6] to classical single-component crystals (metals and semiconductors), i. e., in which the melting point is much higher than the Debye temperature: $T_m > \Theta$. It was when studying the melting of classical crystals that the Lindemann criterion(1) showed good results for substances with different structures at different pressures(P), both for macro- and nanocrystals [1–3]. However, for melting quantum crystals with $T_m < \Theta$, the Lindemann criterion (1) turned out to be not applicable, as it was indicated in the Refs. [16–20]. Therefore, a relatively simple expression for the Lindemann ratio is obtained in this study, which is applicable to both classical (such as metals) and quantum crystals (such as ^{4}He and ^{3}He) at different pressures.

Calculation method

In our works, Refs. [21,22] proposed a delocalization criterion for C–L PT, according to which C–L PT (in the forward and reverse directions) begins when the proportion of delocalized atoms (N_d) will reach a certain value of the total number of atoms in the system (N):

$$x_d(s-l) = \frac{N_d(s-l)}{N} \cong 10^{-2}. \qquad (3)$$

Here $s - l$ means that this value belongs to the solid (s)–liquid (l) transition region, both in the forward and reverse directions. It was shown in Refs. [21,22] that the

delocalization criterion of C–L PT (3) is applicable to both melting and crystallization, and it was shown in Refs. [23,24] that the criterion (3) is also applicable to the liquid-glass transition.

Let us assume for defining the function $x_d(P, T)$ that the atoms in the system can be in two states: localized and delocalized. The atom is localized in the localized state in a cell formed by its nearest neighbors and has only oscillatory degrees of freedom. The atom has access to the entire volume of the system V in the delocalized state, and the atom has only translational degrees of freedom. As it was shown in Refs. [21,22,25], the proportion of delocalized atoms at a given temperature (T) and specific volume ($v = V/N$) is described by the expression:

$$x_d(v, T) = \frac{N_d(v, T)}{N} = \frac{2}{\pi^{1/2}} \int\limits_{E_d/(k_B T)}^{\infty} t^{1/2} \exp(-t) dt, \quad (4)$$

where E_d is the energy required for the transition of an atom from a localized to a delocalized state, k_B is the Boltzmann constant.

Equation (4) is a result of the fact that the number of delocalized atoms having kinetic energy from a certain range of values obeys the Maxwell–Boltzmann distribution which is valid not only to a gas, but also to a liquid, amorphous and crystalline phase [26,27].

The following expression was obtained for the energy of atomic delocalization using the Einstein model for the oscillatory spectrum of a crystal [21,22,25]:

$$E_d = \left(\frac{3}{8\pi^2}\right) m \left(\frac{3ck_B\Theta}{4\hbar k_p^{1/3}}\right)^2 f_y(y_w). \quad (5)$$

Here $\hbar$ — Planck's constant, m — atomic mass, $c = [6k_pV/(\pi N)]^{1/3}$ — distance between the centers of the nearest cells, Θ — Debye temperature, k_p — packing index of a structure of N spherical cells.

The function $f_y(y_w)$ appears in (5) due to the consideration of quantum effects, and it has the following form for a crystal with an oscillatory spectrum according to the Einstein model [25]:

$$f_y(y_w) = \frac{2}{y_w} \frac{[1 - \exp(-y_w)]}{[1 + \exp(-y_w)]}, \quad y_w = \frac{3\Theta}{4T}. \quad (6)$$

It should be noted that if we use the Debye model, then we will obtain the following function instead of the function (6) [25]:

$$f_{yD}(y_D) = \left[\frac{y_D}{4} + D_{n=1}(y_D)\right]^{-1}, \quad y_D = \frac{\Theta}{T},$$

where n-dimensional Debye function defined by the expression:

$$D_n(y_D) = \frac{n}{y_D^n} \int\limits_0^{y_D} \frac{t^n}{\exp(t) - 1} dt.$$

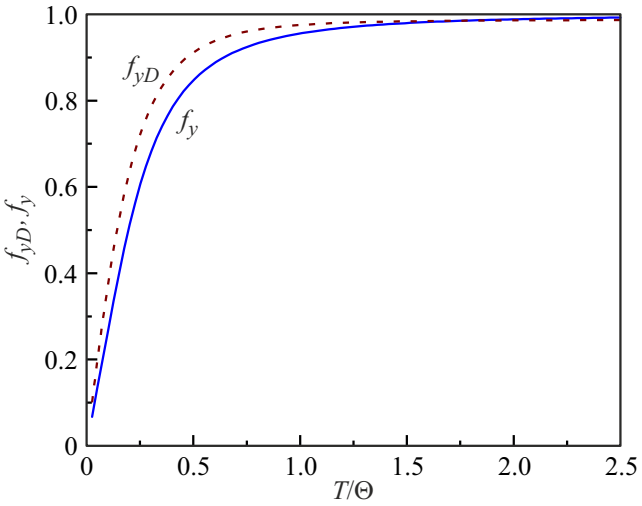

Figure 1. Dependence of functions f_y (solid line) and f_{yD} (dotted line) on relative temperature T/Θ.

Figure 1 shows the dependence of the functions f_y (solid line) and f_{yD} (dotted line) on the relative temperature $T/\Theta = 3/(4y_w)$. Next we will use the formula (6) because we used the Einstein model when we obtained the function E_d from (5). It is easy to see that at $T/\Theta > 1.5$ it is possible to accept: $f_y(T/\Theta > 1.5) \cong 1$. We will call this temperature range the classical one. A linear relationship can be assumed for the function $f_y(y_w)$ at $T/\Theta < 0.4$: $f_y(T/\theta < 0.4) \cong 8T/(3\Theta)$. We will further refer to this temperature range as the quantum one.

Since the delocalization criterion of C–L PT (3) was obtained in Refs. [21,22] for classical crystals (for which $f_y(T_m/\Theta > 1.5) \cong 1$), then it follows from (3)–(5) that the following equation holds in case of melting of a classical crystal:

$$\frac{E_d}{k_B T_m} = \left(\frac{3}{8\pi^2}\right) \frac{k_B m}{T_m} \left(\frac{3c\Theta}{4\hbar k_p^{1/3}}\right)^2 \cong 5.672. \quad (7)$$

A relation follows from the formula (7) that is functionally consistent with the dependence derived from the Lindemann criterion:

$$T_m = \left(\frac{3}{8\pi^2}\right) \frac{k_B m}{5.672} \left(\frac{3c\Theta}{4\hbar k_p^{1/3}}\right)^2 = L_E^2 \, k_B \frac{m}{3} \left(\frac{3c\Theta}{4\pi}\right)^2. \quad (8)$$

It can be seen from (8) that according to the criterion (3) the Lindemann relation for classical crystals (with $T_m > 1.5\Theta$) with an oscillatory spectrum according to the Einstein model is determined by the expression:

$$L_E(T_m > 1.5\Theta) = \left(\frac{9}{8\pi^2 5.672}\right)^{1/2} \frac{1}{k_p^{1/3}} = \frac{0.1418}{k_p^{1/3}}. \quad (9)$$

It can be seen from (9) that for classical crystals the value L_E is determined only by the crystal structure and does not depend on the pressure or the size of the nanocrystal.

Let us summarize (9) for the case of a quantum crystal by comparing the formulas for energy (ε) and the RMS displacement of a classical and quantum n-dimensional harmonic oscillator:

$$\varepsilon_{cl} = \varepsilon_{qn}(T_m > 1.5\Theta) = nk_B T_m, \ \varepsilon_{qn} = \frac{\varepsilon_{cl}}{f_y(y_w)},$$

$$\langle u^2\rangle_{cl} = \langle u^2\rangle_{qn}(T_m > 1.5\Theta), \ \langle u^2\rangle_{qn} = \frac{\langle u^2\rangle_{cl}}{f_y(y_w)}. \quad (10)$$

It can be seen from formulas (10) that the following expression can be assumed for generalizing the formula (9) for the case of a quantum crystal:

$$L_E(T_m) = \frac{0.1418}{k_p^{1/3}[f_y(y_w)]^{1/2}}. \quad (11)$$

The formulas for the delocalization criterion of C–L PT (4) and (7) and for the melting point (8) can be generalized for the case of an arbitrary value T_m/Θ in the following form based on (11):

$$x_d(v, T_m) = \frac{N_d(v, T_m)}{N} = \frac{2}{\pi^{1/2}} \int\limits_{5.672[f_y(y_w)]^2}^{\infty} t^{1/2}\exp(-t)dt,$$

$$\frac{E_d}{k_B T_m} = \left(\frac{3}{8\pi^2}\right)\frac{k_B m}{T_m}\left(\frac{3c\Theta}{4\hbar k_p^{1/3}}\right)^2 f_y(y_w) \cong 5.672[f_y(y_w)]^2,$$

$$T_m = \left(\frac{3}{8\pi^2}\right)\frac{k_B m}{5.672 f_y(y_w)}\left(\frac{3c\Theta}{4\hbar k_p^{1/3}}\right)^2$$

$$= 0.003768\,\frac{k_B m}{f_y(y_w)}\left(\frac{c\Theta}{\hbar k_p^{1/3}}\right)^2. \quad (12)$$

In the quantum domain, i. e. at $T_m < 0.4\Theta$, where $f_y(T_m/\Theta < 0.4) \cong 8T_m/(3\Theta)$ holds, formulas (12) can be simplified to the form:

$$x_d(v, T_m) = \frac{N_d(v, T_m)}{N} = \frac{2}{\pi^{1/2}} \int\limits_{40.334(T_m/\Theta)^2}^{\infty} t^{1/2}\exp(-t)dt,$$

$$\frac{E_d}{k_B T_m} \cong 5.672\left(\frac{8T_m}{3\Theta}\right)^2 = 40.334\left(\frac{T_m}{\Theta}\right)^2, \quad (13)$$

$$L_E(T_m < 0.4\Theta) \cong \frac{0.1418}{k_p^{1/3}}\left(\frac{3\Theta}{8T_m}\right)^{1/2} = \frac{0.0868}{k_p^{1/3}}\left(\frac{\Theta}{T_m}\right)^{1/2},$$

$$T_m = \left[\left(\frac{3}{8\pi^2}\right)\frac{k_B m}{5.672}\left(\frac{3c\Theta}{4\hbar k_p^{1/3}}\right)^2\frac{3\Theta}{8}\right]^{1/2}$$

$$= 0.03759\,\frac{c\Theta}{\hbar k_p^{1/3}}\,(mk_B\Theta)^{1/2}.$$

The following conclusions can be drawn from formulas (11)–(13).

1) The value $L_E(T_m < 0.4\Theta)$ for quantum crystals is determined not only by the crystal structure, but also depends on the ratio Θ/T_m.

2) During the transition from the classical to the quantum domain, the function T_m changes its functional dependence: $T_m \sim (c\Theta)^2$ holds with $T_m > 1.5\Theta$, $T_m \sim c\Theta^{3/2}$ holds with $T_m < 0.4\Theta$.

3) If $T_m/\Theta = 0$ holds, then all the atoms of a quantum crystal are in a delocalized state at the melting point.

As it was shown in Refs. [28,29], the more noticeably the shape of the nanocrystal deviates from the energetically optimal shape the greater is the decrease of function Θ with an isobaric decrease of the nanocrystal size. Therefore, the function $T_m/\Theta \sim c\Theta^{1/2}$ will also decrease as the size of the quantum nanocrystal decreases. Thus, it follows from (13) that the more noticeably the shape of the nanocrystal deviates from the energetically optimal shape the greater is the increase of value L_E for quantum crystals with an isobaric decrease of the nanocrystal size. This is consistent with the results of Ref. [18], which showed by the Monte Carlo diffusion method that the Lindemann ratio increases with the decrease of the nanoparticle size. It should be noted that we showed in Ref. [30] that the delocalization criterion C–L PT (3) is valid for nanoparticles: for nanocrystal melting and for crystallization of a nanodrop. Therefore, the formulas obtained on the basis of criteria (3) are also applicable to the nanocrystal.

We calculated the value $L_E(T_m)$ for both classical and quantum crystals for evaluation of the correctness of the formulas (11) and (13) obtained for L_E and compared the results with estimates obtained by other authors.

2. Calculation results

2.1. Classic crystals

Table 3 shows calculated using the formula (9) The values of the Lindemann ratio for classical crystals with an oscillatory spectrum according to the Einstein model. Calculations were performed for the following structures:

1) face-centered cubic (fcc) and hexagonal close-packed (hcp) structures,

2) body-centered cubic (bcc) structure,

3) simple cubic structure (scs),

4) diamond cubic structure (dcs).

5) for two amorphous packings: dense (dense amorphous packing, dap) and loose (loose amorphous packing, lap). The parameters for the dap and lap structures were determined by us in the paper [31]. As shown in [31], in the area of: $5.855 \le k_n \le 6.2793$ and $0.4 \le k_p \le 0.6237$, one value of the first coordination number k_n corresponds to two or three values of the packing index k_p. Therefore, this structural region was defined in Ref. [31] as the „random packing“ area.

It can be seen from Table 3 that the values we obtained L_E for fcc and bcc structures are slightly higher than the results from studies in Refs. [6–8], and less than the results of study in Ref. [9], which are presented in Table 1. The calculation results provided in Table 3 are in good agreement with the estimates for fcc, hcp, and bcc metals

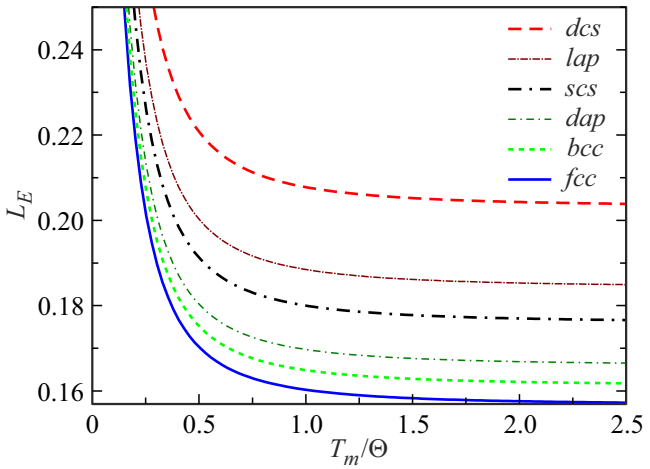

Figure 2. Dependence of the function $L_E(T_m/\Theta)$ for structures from Table 3.

that were obtained in Ref. [16]. Our calculations of value L_E for the diamond structure are in good agreement with the calculations of the Lindemann ratio for silicon (Si) and germanium (Ge) obtained by the perturbation theory method with the local Heine-Abarenkov pseudopotential in Ref. [32]: $L(\mathrm{Si}) = 0.272 \pm 0.03$, $L(\mathrm{Ge}) = 0.249 \pm 0.03$. Our results are also consistent with the results obtained for silicon nanocrystals by the molecular dynamics method:
L (Si with Stillinger-Weber potential) $= 0.19$ [33],
L (Si with Stillinger-Weber potential) $= 0.35-0.39$ for the heating rates of $(5.625-5.113) \cdot 10^{11}$ K/s [34],
L (Si with Tersoff-Agrawal-Raff-Komanduri potential) $= 0.2$ [35].

Our calculations of L_E for dense amorphous packing (dap) are also consistent with the estimates of the Lindemann parameter for softening inorganic glasses, which were obtained in Ref. [24]: $L(\mathrm{Glass–Liquids}) = 0.11-0.15$.

The change of the function $L_E(T_m/\Theta)$ for the classical and quantum temperature ranges was calculated using the formula (11). The calculation result for various structures from Table 3 is shown in Figure 2. It can be seen that the function L_E has different dependencies for the classical ($T_m/\Theta > 1.5$) and quantum (at $T_m/\Theta < 0.4$) temperature ranges, for which the following asymptotic expressions can

Table 3. Values of the Lindemann ratio for classical crystals: k_n and k_p — the first coordination number and packing index of the structure

Structure	k_n	k_p	L_E
fcc and hcp structures	12	0.7405	0.1567
bcc structure	8	0.6802	0.1612
Dense amorphous packing (dap)	6.2793	0.62370	0.1660
Simple cubic structure (scs)	6	0.5236	0.1759
Loose amorphous packing (lap)	6.2793	0.45556	0.1843
Diamond cubic structure (dcs)	4	0.3401	0.2031

Table 4. Experimental data for fcc crystals of inert gases at $P = 1$ bar and calculated values of the Lindemann ratio based on them and using the formula (11)

Crystal	m, a.m.u.	T_m, K	Θ, K	Ref.	T_m/Θ	L_E
Ne	20.18	24.56	66.6	[36]	0.369	0.1802
		24.57	74.6	[37]	0.329	0.1854
Ar	39.95	83.81	93.3	[36]	0.8983	0.1611
		83.78	93.3	[37]	0.8980	0.1611
Kr	83.30	115.78	71.7	[36]	1.615	0.1581
		115.95	71.7	[37]	1.617	0.1581
Xe	131.3	161.37	55.0	[36]	2.934	0.1571
		161.36	64.0	[37]	2.521	0.1573

be used:

$$L_E(T_m) = \frac{0.1418}{k_p^{1/3}[f_y(y_w)]^{1/2}} \cong \frac{0.1418}{k_p^{1/3}} \begin{cases} 1 - \frac{y_m}{4} = 1 - \frac{3\Theta}{16T_m}, & \text{for } \frac{T_m}{\Theta} > 1.5 \\ \left(\frac{y_m}{2}\right)^{1/2} = \left(\frac{3\Theta}{8T_m}\right)^{1/2}, & \text{for } \frac{T_m}{\Theta} < 0.4 \end{cases}.$$

2.2. Crystals of inert gases

A transition from a classical type crystal (Kr and Xe) to a quantum type crystal (Ne) takes place in the group of fcc crystals of inert gases. Therefore, we calculated the value L_E for these crystals using the formula (11). The melting point and Debye temperature experimentally determined for crystals of inert gases at atmospheric pressure ($P = 1$ bar) are provided in Table 4, as well as the values of the Lindemann ratio calculated from them using the formula (11) for crystals with an oscillatory spectrum according to the Einstein model. The upper values are taken from Ref. [36] in each line, and the lower values are from the article in Ref. [37].

It can be seen from Table 4 that our calculations are in good agreement with the results from Ref. [14], but slightly exceed the estimates of other authors, which are provided in Table 2.

2.3. Crystals of hydrogen isotope molecules

Table 5 shows the melting point and Debye temperature experimentally determined at various pressures for molecular hcp crystals of hydrogen isotopes: para-hydrogen, p-H_2, $m = 2.016$ a.m.u. and ortho-deuterium, o-D_2, $m = 4.028$ a.m.u. The Lindemann ratios for crystals with an oscillatory spectrum according to the Einstein model were calculated based on these data using formula (11). It can be seen from Table 5 that our calculations are in good agreement with theoretical and experimental

Table 5. Experimental data determined at different pressures for *hcp* crystals of hydrogen isotopes and calculated using them and formula (11) values of the Lindemann ratio

Crystal	P, bar	T_m, K	Θ, K	T_m/Θ	L_E
p-H_2	1	13.96 [37]	118.0 [38]	0.1183	0.2795
	400	25 [39,40]	122.9 [39]	0.2034	0.2182
			151.1 [40]	0.1655	0.2384
o-D_2	1	18.72 [33]	114.0 [38]	0.1642	0.2393
	200	25 [35,36]	91.2 [39]	0.2741	0.1956
			109.0 [40]	0.2294	0.2081

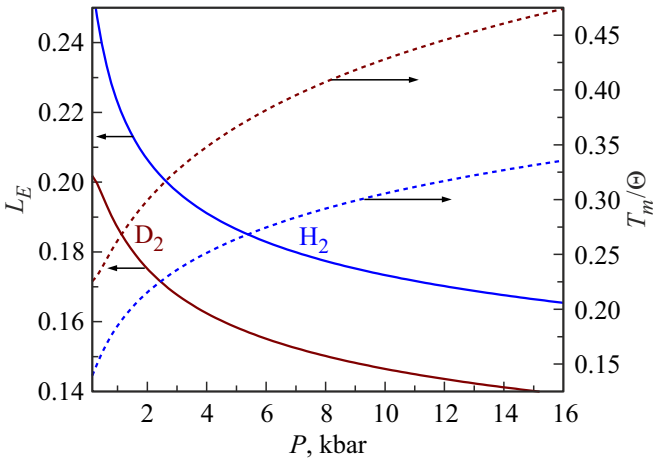

Figure 3. Baric dependence of the ratio T_m/Θ (dotted lines, right scale) and the function L_E (solid lines, left scale). The lower solid curve for L_E and the upper dotted curve for T_m/Θ refer to D_2.

estimates from Refs. [17–40,41,42], where the following was obtained: $L(\text{p-H}_2) \cong 0.2$.

Approximations of experimental baric dependences (up to 19 kbar) for the melting point and Debye temperature were obtained Ref. [40] in the form of equations of the following form (here T_m and Θ in K, P in kbar):
for p-H_2

$$T_m = \left(\frac{P + 0.2442}{2.858 \cdot 10^{-3}}\right)^{1/1.724}, \qquad (14)$$

$$\Theta = 85.389 - 0.729P_m + 98.832P_m^{0.481},$$

for o-D_2

$$T_m = \left(\frac{P + 0.5431}{3.66 \cdot 10^{-3}}\right)^{1/1.677}, \qquad (15)$$

$$\Theta = 74.65 + 65.298P_m^{0.476}.$$

We used the dependencies (14) and (15) to calculate the baric dependence of the functions T_m/Θ and L_E which are shown in Figure 3. It can be seen from these dependences that the Lindemann ratio for molecular *hcp* crystals of hydrogen isotopes decreases with the increase of pressure.

2.4. Crystals of helium isotopes

Helium has two stable isotopes ^{3}He ($m = 3.016$ a.m.u.) and ^{4}He ($m = 4.0026$ a.m.u.). Experimental data for crystals of helium isotopes with *bcc* and *hcp* structures from Refs. [43,44] are shown in Table 6, where V is the molar volume of the crystal, $T_m(1)$ and $T_m(2)$ are the upper and lower crystallization temperatures, Θ is the Debye temperature at $T = 0$ K. Using these values and the formula (13), the Lindemann ratios for crystals with an oscillatory spectrum were calculated according to the Einstein model, which are presented in Table 6.

It has been shown in theoretical papers by other authors that for quantum systems such as helium and the electronic Wigner crystal, the Lindemann ratio should be at least: 0.3 [19], $0.267 \pm 0.0026 = 0.2644-0.2696$ [45], $L(bcc\text{-}^3\text{He}) = 0.368$ and $L(bcc\text{-}^4\text{He}) = 0.292$ [46]. The following was obtained in Ref. [41] using the Quantum Monte Carlo simulations for *bcc* structures ^{3}He at $T_m = 0.65$ K and ^{4}He at $T_m = 1.6$ K : $L(bcc\text{-}^3\text{He}) = 0.344$, $L(bcc\text{-}^4\text{He}) = 0.291$. The RMS displacement of an atom in a *hcp* crystal ^{4}He at $T = 0.7 \pm 0.05$ was experimentally measured in Ref. [47]. The following was obtained in Ref. [47]: $L(hcp\text{-}^4\text{He}) = 0.262 \pm 0.006$. It can be seen from Table 6 that the calculated value L_E is consistent with the estimates from Refs. [19,41,45–47]. The value of the Lindemann ratio decreases as the molar volume of the *bcc* or *hcp* of a helium crystal decreases (i. e., with the increase of pressure). It is also seen from Table 6 that the value L_E is greater at the upper crystallization temperature than at the lower one crystallization temperature.

Many authors (for example, in Refs. [17,18,36,37,46,48]) pointed out the connection of the Lindemann relation with the de Boer parameter [49](Λ), which characterizes the role of quantum effects in the energy of a crystal, and which has the form:

$$\Lambda = \frac{2\pi\hbar}{\sigma(mD)^{1/2}}. \qquad (16)$$

Here σ is the distance between atoms at which the paired interatomic potential (2) becomes zero: $\varphi(\sigma) = 0$.

Figure 4 shows the dependences of the Lindemann ratio calculated for crystals of hydrogen isotopes and inert gases on the de Boer parameter from Refs. [18,47,49], which are shown in Table 7. The value of the de Boer parameter in later works differs from the value (Λ_B) that was presentedin Ref. [49] due to the use of different values of the functions of equation (16). Therefore, the values of the de Boer parameter from Ref. [47] (Λ_Z) and from Ref. [18] (Λ_G) are presented in Table 7 along with Λ_B.

As can be seen from Figure 4, the dependence $L_E(\Lambda_i)$ for crystals of hydrogen isotopes and inert gases with a large correlation coefficient (R) is approximated by a linear

Table 6. Experimental data for helium isotope crystals with *bcc* and *hcp* structures from Refs. [43,44] and calculated values L_E

Crystal	V, cm^3/mol	$T_m(1)$, K	$T_m(2)$, K	Θ, K	Ref.	$T_m(1)/\Theta$	$L_E(1)$	$T_m(2)/\Theta$	$L_E(2)$
bcc-^{3}He	23.80	1.276	0.898	20.10	[43]	0.0635	0.3917	0.0447	0.4668
	20.18	2.874	2.417	28.99	[43]	0.0991	0.3135	0.0834	0.3418
hcp-^{3}He	19.05	2.983	2.790	39.20	[43]	0.0761	0.3478	0.0712	0.3596
	11.42	19.33	11.42	128.19	[43]	0.1508	0.2471	0.0891	0.3214
hcp-^{4}He	12.23	16.78	14.23	95.50	[43]	0.1757	0.2289	0.1490	0.2486
	12.21	14.12	16.85	84.0	[44]	0.1681	0.2340	0.2006	0.2143
	21.04	2.27	1.45	24.2	[44]	0.0938	0.3133	0.0599	0.3920

Table 7. The calculated Lindemann ratio (from Tables 4 and 5) and the de Boer parameter from Refs. [18,47,49]

Crystal	m, a.m.u.	L_E(calc)	Λ_B [49] de Boer–1948	Λ_Z [47] Zucker–1961	Λ_G [18] Guardiola–2011
^{3}He	3.0160		3.04*	3.09	0.491*
^{4}He	4.0026		2.64	2.68	0.426
H_2	2.016	0.2795	1.73	1.73	0.293
D_2	4.028	0.2393	1.22	1.22	0.207
Ne	20.18	0.1802–0.1854	0.591	0.574	0.094
Ar	39.95	0.1611	0.187	0.184	0.029
Kr	83.3	0.1581	0.102	0.102	0.016
Xe	131.3	0.1571–0.1573	0.0636	0.062	0.010

Note. * Calculated using the formula: $\Lambda(^3\text{He}) = \Lambda(^4\text{He})[m(^4\text{He})/m(^3\text{He})]^{1/2} = 1.152\Lambda(^4\text{He})$.

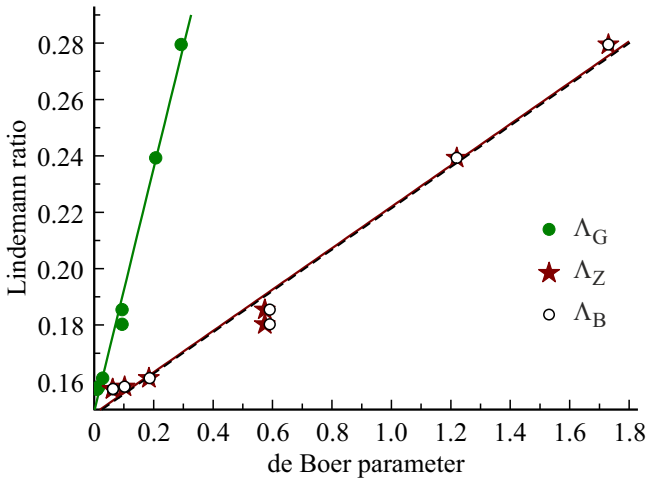

Figure 4. Dependence of the calculated Lindemann ratio on the de Boer parameter from Refs. [18,47,49].

function of the following form:

$$L_E = 0.14829 + 0.07326\Lambda_B, \quad R = 0.98323,$$

$$L_E = 0.14856 + 0.07336\Lambda_Z, \quad R = 0.98606,$$

$$L_E = 0.14928 + 0.43162\Lambda_G, \quad R = 0.98866. \qquad (17)$$

Calculations using linear approximations (7) for crystals from helium isotopes have shown the following:

the following is obtained from Λ_B:

$$L_E(^3\text{He}) = 0.3710, \quad L_E(^4\text{He}) = 0.3417,$$

the following is obtained from Λ_Z:

$$L_E(^3\text{He}) = 0.3752, \quad L_E(^4\text{He}) = 0.3452,$$

the following is obtained from Λ_G:

$$L_E(^3\text{He}) = 0.3612, \quad L_E(^4\text{He}) = 0.3332.$$

These results confirm the correctness of both the results of our calculations for helium crystals from Table 6 and the correctness of the used formulas (11) and (13).

In conclusion, we would like to note that the effect of the anharmonicity of atomic vibrations in a crystal on the melting parameters of both classical [3,50–52] and quantum [20,53] crystals is insignificant. That is why the use of the Einstein model of independent harmonic oscillators in this work has shown good results. We showed that melting is attributable to delocalization of definite portion of atoms of both macro- [{]21,22}, and nanocrystal [29,30].

3. Conclusion

A relatively simple method for calculating the Lindemann ratio is proposed based on C–L PT delocalization criterion and the Einstein crystal model, which can be applied to both classical and quantum crystals.

It is shown that the Lindemann ratio is determined only by the crystal structure for single-component classical crystals (in which $T_m/\Theta > 1.5$). Calculations for various structures of classical crystals have shown good agreement with the estimates of other authors.

It is shown that the Lindemann relation is determined for quantum single-component crystals (in which $T_m/\Theta < 0.4$) by both the crystal structure and the function Θ/T_m. This leads to the fact that the Lindemann ratio for quantum crystals decreases with the increase of pressure along the melting line. The more noticeable is the deviation of the shape of the nanocrystal from the energetically optimal shape the greater is the increase of the Lindemann ratio for quantum nanocrystals with an isobaric decrease of the size of the nanocrystal.

The function $T_m(c, \Theta)$ changes its functional dependence in case of the transition from the classical to the quantum domain. Therefore, the use of the Lindemann criterion to study the melting of quantum crystals (as the authors tried to do in Ref. [20] when studying the melting of atomic metallic hydrogen) showed incorrect results.

A generalization of the delocalization melting criterion for the case of single-component quantum crystals is obtained. It is shown that all the atoms of a quantum crystal are in a delocalized state at the melting point if the following condition holds: $T_m/\Theta = 0$.

Acknowledgments

The author would like to thank S.P. Kramynin, K.N. Magomedov, N.Sh. Gazanova, Z.M. Surkhayeva and M.M. Gadzhieva for fruitful discussions and assistance in work.

Conflict of interest

The author declares that he has no conflict of interest.

References

[1] J.H. Bilgram. Phys. Rep. **153**, *1*, 1–89 (1987). DOI: 10.1016/0370-1573(87)90047-0
[2] Q.S. Mei, K. Lu. Prog. Mater Sci. **52**, *8*, 1175–1262 (2007). DOI: 10.1016/j.pmatsci.2007.01.001
[3] G. de With. Chem. Rev. **123**, *23*, 13713–13795 (2023). DOI: 10.1021/acs.chemrev.3c00489
[4] F.A. Lindemann. Phys. Z. **11**, *14*, 609–612 (1910).
[5] J.J. Gilvarry. Phys. Rev. **102**, *2*, 308–316 (1956). DOI: 10.1103/PhysRev.102.308
[6] J.J. Gilvarry. Phys. Rev. **103**, *6*, 1700–1704 (1956). DOI: 10.1103/PhysRev.103.1700
[7] J.N. Shapiro. Phys. Rev. B **1**, *10*, 3982–3989 (1970). DOI: 10.1103/PhysRevB.1.3982
[8] S.A. Cho. J. Phys. F. Met. Phys. **12**, *6*, 1069–1083 (1982). DOI: 10.1088/0305-4608/12/6/008
[9] T. Matsuura, H. Suzuki, K.I. Takano, F. Honda. J. Phys. Soc. Jpn. **79**, *5*, 053601 (2010). DOI: 10.1143/JPSJ.79.053601
[10] M.M. Vopson, N. Rogers, I. Hepburn. Solid State Commun. **318**, 113977 (2020). DOI: 10.1016/j.ssc.2020.113977
[11] V.V. Goldman. J. Phys. Chem. Solids **30**, *4*, 1019–1021 (1969). DOI: 10.1016/0022-3697(69)90301-1
[12] N.P. Gupta. Solid State Commun. **13**, *1*, 69–71 (1973). DOI: 10.1016/0038-1098(73)90069-0
[13] R.K. Crawford. Melting, vaporization and sublimation. In „Rare Gas Solids“, Eds. M.L. Klein, J.A. Venables. Academic Press, New York (1977) Vol. 2, P. 663–728.
[14] R.K. Singh, D.K. Neb. Phys. Status Solidi B **126**, *1*, K15–K18 (1984). DOI: 10.1002/pssb.2221260153
[15] P. Mohazzabi, F. Behroozi. J. Mater. Sci. Lett. **6**, 404–406 (1987). DOI: 10.1007/BF01756777
[16] S.S. Batsanov. Russ. J. Phys. Chem. A **83**, *11*, 1836–1841 (2009). DOI: 10.1134/S0036024409110053
[17] C. Domb. II Nuovo Cimento (1955–1965) **9**, (Suppl 1), 9–26 (1958). DOI: 10.1007/BF02824224
[18] R. Guardiola, J. Navarro. J. Phys. Chem. A **115**, *25*, 6843–6850 (2011). DOI: 10.1021/jp1111313
[19] S.T. Chui. Phys. Rev. B **41**, *1*, 796–798 (1990). DOI: 10.1103/PhysRevB.41.796
[20] I. Loa, F. Landgren. J. Phys.: Condens. Matter **36**, *18*, 185401 (2024). DOI: 10.1088/1361-648X/ad1e08
[21] M.N. Magomedov. Tech. Phys. Lett. **33**, *10*, 837–840 (2007). DOI: 10.1134/S1063785007100094
[22] M.N. Magomedov. Phys. Met. Metallogr. **105**, *2*, 116–125 (2008). DOI: 10.1134/S0031918X08020038
[23] D.S. Sanditov. J. Exp. Theor. Phys. **115**, *1*, 112–124 (2012). DOI: 10.1134/S1063776112060143
[24] D.S. Sanditov, B.S. Sydykov. Tech. Phys. **59**, *5*, 682–685 (2014). DOI: 10.1134/S1063784214050272
[25] M.N. Magomedov. Phys. Met. Metallogr. **74**, *4*, 319–321 (1992).
[26] A.G. Chirkov, A.G. Ponomarev, V.G. Chudinov. Tech. Phys. **49**, *2*, 203–206 (2004). DOI: 10.1134/1.1648956
[27] G.M. Poletaev, M.D. Starostenkov. Phys. Solid State **51**, *4*, 727–732 (2009). DOI: 10.1134/S106378340904012X
[28] M.N. Magomedov. Crystallogr. Rep. **62**, *3*, 480–496 (2017). DOI: 10.1134/S1063774517030142
[29] M.N. Magomedov. Phys. Solid State **66**, *2*, 221–233 (2024). DOI: 10.61011/PSS.2024.02.57919.241
[30] M.N. Magomedov. Tech. Phys. **55**, *9*, 1373–1377 (2010). DOI: 10.1134/S1063784210090227
[31] M.N. Magomedov. Tech. Phys. **65**, *10*, 1659–1665 (2020). DOI: 10.1134/S1063784220100138
[32] T. Soma, H. Matsuo. J. Phys. C: Solid State Phys. **15**, *9*, 1873–1882 (1982). DOI: 10.1088/0022-3719/15/9/010
[33] N.T.T. Hang. Commun. in Phys. **24**, *3*, 207–215 (2014). DOI: 10.15625/0868-3166/24/3/4070
[34] L.V. Sang, V.V. Hoang, D.T.N. Tranh. Eur. Phys. J. D **69**, 208 (2015). DOI: 10.1140/epjd/e2015-60153-1
[35] H. Li, R. Xu, Z. Bi, X. Shen, K. Han. J. Electron. Mater. **46**, *7*, 3826–3830 (2017). DOI: 10.1007/s11664-016-5070-8
[36] G.L. Pollack. Rev. Mod. Phys. **36**, *3*, 748–791 (1964). DOI: 10.1103/RevModPhys.36.748
[37] Cryocrystals, Eds. B.I. Verkin, A.F. Prikhod'ko. Naukova Dumka, Kiev (1983). 526 p. (in Russian)
[38] M. Nielsen. Phys. Rev. B **7**, *4*, 1626–1635 (1973). DOI: 10.1103/PhysRevB.7.1626
[39] D.A. Young, M. Ross. J. Chem. Phys. **74**, *12*, 6950–6955 (1981). DOI: 10.1063/1.441058
[40] V. Diatschenko, C.W. Chu, D.H. Liebenberg, D.A. Young, M. Ross, R.L. Mills. Phys. Rev. B **32**, *1*, 381–389 (1985). DOI: 10.1103/PhysRevB.32.381
[41] M. Dusseault, M. Boninsegni. Phys. Rev. B **95**, *10*, 104518 (2017). DOI: 10.1103/PhysRevB.95.104518

[42] T.R. Prisk, R.T. Azuah, D.L. Abernathy, G.E. Granroth, T.E. Sherline, P.E. Sokol, J. Hu, M. Boninsegni. Phys. Rev. B **107**, *9*, 094511 (2023). DOI: 10.1103/PhysRevB.107.094511
[43] H.H. Sample, C.A. Swenson. Phys. Rev. **158**, *1*, 188–199 (1967). DOI: 10.1103/PhysRev.158.188
[44] E.C. Heltemes, C.A. Swenson. Phys. Rev. **128**, *4*, 1512–1519 (1962). DOI: 10.1103/PhysRev.128.1512
[45] P.A. Whitlock, D.M. Ceperley, G.V. Chester, M.H. Kalos. Phys. Rev. B **19**, *11*, 5598–5633 (1979). DOI: 10.1103/PhysRevB.19.5598
[46] H.R. Glyde. „Helium, Solid". P. 1–11. [Online]. http://www.physics.udel.edu/ glyde/Solid_H13.pdf
[47] C.A. Burns, E.D. Isaacs. Phys. Rev. B **55**, *9*, 5767–5771 (1997). DOI: 10.1103/PhysRevB.55.5767
[48] I.J. Zucker. Proc. Phys. Soc. **77**, *4*, 889–900 (1961). DOI: 10.1088/0370-1328/77/4/311
[49] J. De Boer. Physica **14**, *2–3*, 139–148 (1948). DOI: 10.1016/0031-8914(48)90032-9
[50] B. Grabowski, L. Ismer, T. Hickel, J. Neugebauer. Phys. Rev. B **79**, *13*, 134106 (2009). DOI: 10.1103/PhysRevB.79.134106
[51] C. Freysoldt, B. Grabowski, T. Hickel, J. Neugebauer, G. Kresse, A. Janotti, C.G. Van de Walle. Rev. Mod. Phys. **86**, *1*, 253–305 (2014). DOI: 10.1103/RevModPhys.86.253
[52] D.D. Satikunvar, N.K. Bhatt, B.Y. Thakore. J. Appl. Phys. **129**, *3*, 035107 (2021). DOI: 10.1063/5.0022981
[53] M. Borinaga, I. Errea, M. Calandra, F. Mauri, A. Bergara. Phys. Rev. B **93**, **17**, 174308 (2016). DOI: 10.1103/PhysRevB.93.174308

Translated by EgoTranslating